Effects of molybdena on the catalytic properties of vanadia domains supported on alumina for oxidative dehydrogenation of propane

Hongxing Dai, Alexis T. Bell,* and Enrique Iglesia *

Chemical Sciences Divisions, Lawrence Berkeley National Laboratory, Department of Chemical Engineering, University of California, Berkeley, CA 94720-1462, USA

Abstract

The oxidative dehydrogenation (ODH) of propane was investigated on vanadia dispersed on alumina containing a nominal polymolybdate monolayer (4.8 Mo/nm^2). Dehydrogenation rates and selectivities on these catalysts were compared with those on vanadia domains dispersed on alumina. At a given vanadia surface density, ODH reaction rates per gram of catalyst were about 1.5–2 times greater on MoO_x-coated Al_2O_3 than on pure Al_2O_3 supports. The higher activity of vanadia dispersed on MoO_x-coated Al_2O_3 reflects the greater reducibility of VO_x species as a result of the replacement of V–O–Al with V–O–Mo bonds. The MoO_x interlayer also increased the alkene selectivity by inhibiting propane and propene combustion rates relative to ODH rates. This appears to reflect a smaller number of unselective V_2O_5 clusters when alkoxide precursors are used to disperse vanadia on MoO_x/Al_2O_3 as compared to the use of metavanadate precursor to disperse vanadia on pure Al_2O_3. At 613 K, the ratio of rate coefficients for propane combustion and propane ODH was three times smaller on MoO_x/Al_2O_3 than on Al_2O_3 supports. The ratio of rate constants for propene combustion and propane ODH decreased by a similar factor.
© 2003 Elsevier Inc. All rights reserved.

Keywords: Propane; Oxidative dehydration; Vanadia

1. Introduction

Oxidative dehydrogenation (ODH) of propane to propene is an attractive alternative to nonoxidative routes, because ODH reactions are favored by thermodynamics even at low temperatures and do not lead to the formation of coke and lower molecular weight products. Among the many materials examined as catalysts for propane ODH, vanadia- and molybdena-based materials remain among the most effective [1–15]. Investigations of propane ODH on Al_2O_3- and ZrO_2-supported VO_x and MoO_x have shown that the highest specific activity (per V or Mo atom) for C_3H_8 ODH is achieved at near-monolayer coverages of polyvanadate (7.5 V/nm^2) or polymolybdate (4.8 Mo/nm^2) species on these supports [12–15]. UV–visible studies of supported vanadia and molybdena domains have shown that there is a strong correlation between the specific activity for ODH and the absorption-band-edge energy. For each oxide, the reaction turnover rate increases as the absorption-edge energy decreases. This trend is related mechanistically to the redox cycles involving lattice oxygen responsible for propane ODH [15]. Consistent with this picture, it is observed that for a given equivalent submonolayer surface coverage of the support, the propane ODH activity for dispersed vanadia is higher than that for dispersed molybdena. At oxide coverages above a monolayer, the specific activity of both oxides decreases because an increasing fraction of the deposited oxide is present within three-dimensional particles, and, hence, some of the Mo and V atoms are inaccessible for catalysis.

The effects of oxide coverage on the selectivity to propene can be described in terms of the following reaction scheme [1,3,4,9–11,13,14]:

$$C_3H_8 \xrightarrow{k_1} C_3H_6$$
$$C_3H_8 \xrightarrow{k_2} CO_x \xleftarrow{k_3} C_3H_6$$
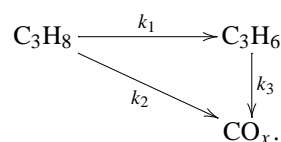
The rate coefficients k_1, k_2, and k_3 describe the rates of propane ODH, propane combustion, and propene combustion, respectively. Values of these coefficients can be obtained by analysis of reaction rates as a function of reactant

* Corresponding authors.
E-mail addresses: bell@cchem.berkeley.edu (A.T. Bell),
iglesia@cchem.berkeley.edu (E. Iglesia).

space velocity [7,10,13,14]. Studies of alumina-supported molybdena have shown that both k_2/k_1 and k_3/k_1 ratios decreased as the surface density of molybdena increased, suggesting that the presence of Mo–O–Al surface sites favors the adsorption of propene and the combustion of the resulting alkoxides [13]. In contrast with molybdena, the values of k_2/k_1 and k_3/k_1 ratios on alumina-supported vanadia increased with increasing oxide surface coverage, apparently as a result of lower selectivity on three-dimensional vanadia clusters than on monomers and two-dimensional oligomers [14]. Thus, while monolayer coverage of alumina by vanadia results in high specific propane ODH activity, it also leads to lower propene selectivities.

The preceding discussion suggests that in order to attain high propane ODH activity and selectivity, the reducibility of vanadia must be increased while minimizing the formation of V_2O_5 crystallites, which lead to low propene selectivity. An approach to achieve this goal is to disperse VO_x in small domains on an oxide that is less reducible than vanadia, but more reducible than the alumina support (e.g., $V_2O_5/MoO_3/Al_2O_3$). While Gao and co-workers [16–18] have reported higher methanol oxidation rates on bilayer $V_2O_5/TiO_2/SiO_2$ and $V_2O_5/ZrO_2/SiO_2$ structures than on V_2O_5/SiO_2, to the best of our knowledge, similar catalysts have not been examined for alkane ODH. The most relevant previous study is by Ueda et al. [19], who have investigated bulk V–M–O mixed metal oxides (M = Al, Fe, Cr, and Ti) as ethane ODH catalysts; these authors did not explore similar compositions as bilayer oxide structures. Here, we report the preparation and structural characterization of vanadia dispersed on a monolayer of molybdena on alumina and the activity and selectivity of such materials for propane ODH. We show that a molybdena interlayer enhances ODH activity of dispersed vanadia and also suppresses propane and propene combustion side reactions.

2. Experimental

The 10.5 wt% V_2O_5/Al_2O_3 and 12 wt% MoO_3/Al_2O_3 catalysts were prepared by incipient wetness impregnation of γ-Al_2O_3 (Degussa, AG, 100 m^2/g) with a solution of ammonium metavanadate (Aldrich, 99%) and oxalic acid (NH_4VO_3:oxalic acid 1:2 molar ratio) and ammonium heptamolybdate (Aldrich, 99%), respectively. The samples were dried overnight at 398 K before thermal treatment at 573 K in a flow of dry air (Airgas, zero grade) for 3 h. Samples with 2–18 wt% V_2O_5 deposited on a 12 wt% MoO_3/Al_2O_3 sample were prepared using previously described methods [16]. After thermal treatment, the 12% MoO_3/Al_2O_3 sample was dried at 393 K for 1 h and then transferred into a N_2-purged glove box. It was then impregnated with a solution of vanadyl isopropoxide (Aldrich, 98%) in isopropanol, kept in the glove box overnight, and transferred into a quartz tube. This procedure was used to avoid hydrolysis of the alkoxide by ambient moisture. These samples were treated

in flowing N_2 at 393 K for 1 h, then at 573 K for 1 h, subsequently treated in flowing dry air at 573 K for 1 h, and finally at 773 K for 2 h. The samples were pressed into wafers, crushed, and sieved to retain particles with 0.18–0.36 mm diameters. Vanadyl isopropoxide was chosen as the vanadium precursor because it led to a higher dispersion of vanadia than by aqueous impregnation of 12 wt% MoO_3/Al_2O_3 with ammonium vanadate. BET surface areas were measured using nitrogen physisorption at its normal boiling point and a Quantasorb surface analyzer (Quantachrome Corp.). Raman spectra were recorded at ambient temperature using a rotating stage quartz cell after samples were treated in dry air at 723 K for 1 h within the cell [13,14].

Propane ODH rates were measured in a quartz microreactor using 0.02–0.04 g of catalyst diluted with equal amounts of quartz powder (40–80 mesh) in order to minimize temperature gradients. Propane (Airgas, 99.9%) and O_2 (Airgas, 99.999%) were used as reactants and He (Airgas, 99.999%) was used as an inert diluent. The partial pressure of propane was 13.5 kPa and that of oxygen, 1.7 kPa, and rate measurements were carried out at 583–703 K. The effluent from the reactor was analyzed with a Hewlett-Packard 6890 gas chromatograph [7,8]. Reactor residence times were varied by changing the reactant flow rates; the resulting propane and oxygen conversions were kept below 2% and 20%, respectively, in all experiments.

3. Results and discussion

BET surface areas and nominal MO_x (M = V, Mo) surface densities are shown in Table 1 for all samples. MO_x surface densities are reported as the number of M atoms per BET surface area (M/nm^2). Two-dimensional MO_x oligomers form a monolayer on Al_2O_3 at 7.5 V/nm^2 [20] and 4.8 Mo/nm^2 [21–23]. The sample designated as 12Mo/Al and used as the coated support has a Mo surface density of 4.8 Mo/nm^2, corresponding to an equivalent polymolybdate monolayer. The addition of vanadia to the surface of 12Mo/Al monotonically decreased BET surface areas. However, most of the observed change is merely due to the increase in catalyst mass upon addition of vanadia. When the BET area was calculated on the basis of the amount of support, Table 1 shows that the decrease in surface area with addition of vanadia is significantly smaller. The sample designated as 10V/12Mo/Al has an apparent surface density of 7.5 V/nm^2, which corresponds to an equivalent polyvanadate monolayer on Al_2O_3. The dispersion of vanadia directly onto alumina causes a reduction in the BET surface area similar to that observed when vanadia is dispersed onto a monolayer equivalent of molybdena on alumina. The sample designated as 10.5V/Al also has an apparent vanadium surface density corresponding to about one polyvanadate monolayer (7.5 V/nm^2).

The Raman spectra of samples treated in dry air at 723 K for 1 h are shown in Fig. 1. The spectrum of 10.5V/Al

Table 1
Surface areas and MO_x (M = V or Mo) surface densities of catalysts

Catalyst composition	Catalyst name	Surface area (m^2/g$_{cat}$)	Surface area (m^2/g$_{support}$[a])	VO$_x$ surface density (V/nm^2)
12 wt% MoO$_3$/Al$_2$O$_3$	12Mo/Al	104	–	4.8 (Mo/nm^2)
10.5 wt% V$_2$O$_5$/Al$_2$O$_3$	10.5V/Al	92	–	7.6
2 wt% V$_2$O$_5$/12 wt% MoO$_3$/Al$_2$O$_3$	2V/12Mo/Al	108	110	1.2
4 wt% V$_2$O$_5$/12 wt% MoO$_3$/Al$_2$O$_3$	4V/12Mo/Al	104	108	2.5
6 wt% V$_2$O$_5$/12 wt% MoO$_3$/Al$_2$O$_3$	6V/12Mo/Al	98	104	4.1
8 wt% V$_2$O$_5$/12 wt% MoO$_3$/Al$_2$O$_3$	8V/12Mo/Al	93	101	5.7
10 wt% V$_2$O$_5$/12 wt% MoO$_3$/Al$_2$O$_3$	10V/12Mo/Al	88	98	7.5
12 wt% V$_2$O$_5$/12 wt% MoO$_3$/Al$_2$O$_3$	12V/12Mo/Al	78	89	10.2
18 wt% V$_2$O$_5$/12 wt% MoO$_3$/Al$_2$O$_3$	18V/12Mo/Al	70	85	17.0

[a] Support = 12 wt% MoO$_3$/Al$_2$O$_3$.

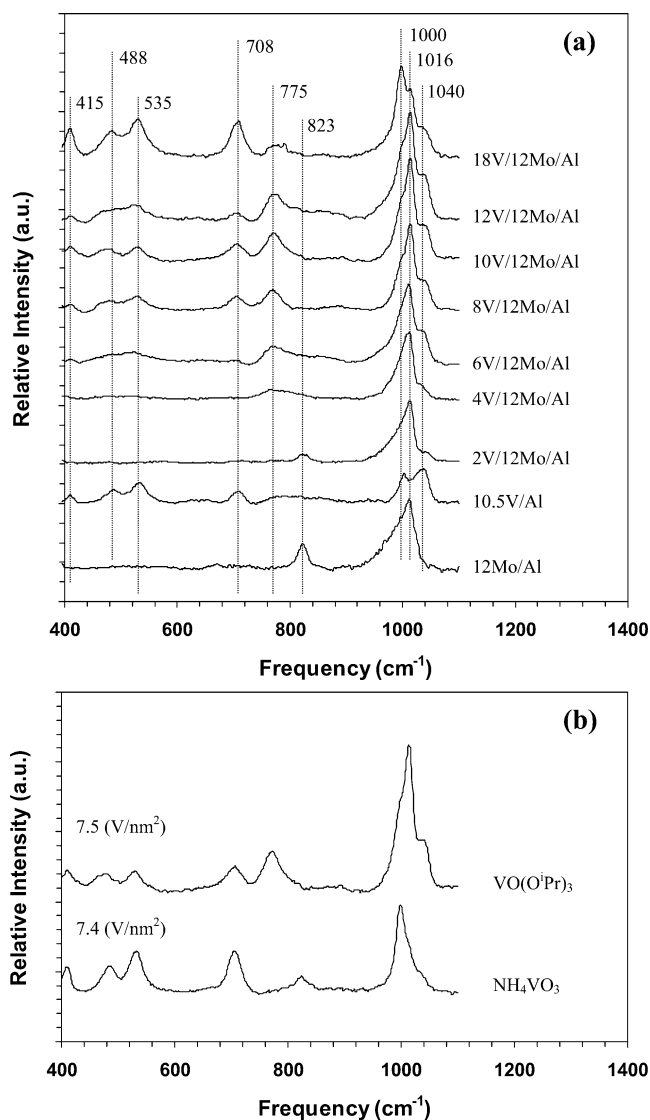

Fig. 1. (a) Raman spectra of 12Mo/Al, 10.5V/Al, and xV/12Mo/Al (x = 2–18). (b) Raman spectra of a monolayer of vanadia dispersed on 12Mo/Al, prepared from VO(O^{i}Pr) and NH$_4$VO$_3$.

weaker bands at 1000, 708, 535, 488, and 412 cm^{-1} arising from V$_2$O$_5$ crystallites [14,24–28]. In view of the much larger Raman scattering cross section of crystalline V$_2$O$_5$ relative to dispersed monovanadate and polyvanadate structures [28], we conclude that these samples contain only traces of crystalline V$_2$O$_5$.

The dehydrated 12Mo/Al sample shows a broad band at 1016 cm^{-1}, a weaker band at 822 cm^{-1}, and a broad feature at 673 cm^{-1}. Previous studies of MoO$_3$/Al$_2$O$_3$ samples have assigned bands at 955–1010 cm^{-1} to MoO$_x$ oligomers and bands at 999, 822, and 673 cm^{-1} to MoO$_3$ crystallites [13,29–31]. Since the Raman cross section for MoO$_3$ is larger than that for monovanadate and polyvanadate species, these data indicate that most of the molybdena covers the surface of the alumina. The deposition of vanadia onto 12Mo/Al leads to Raman bands characteristic of various vanadia structures for vanadia contents higher than 2 wt% (> 1.2 V/nm^2) (Fig. 1a). The band at 1040 cm^{-1} corresponds to V=O vibrations in isolated monovanadate species. For 4V/12Mo/Al, a well-defined band appears at 775 cm^{-1}, which is assignable to either V–O–V vibrations of polyvanadate species [24,25,32], or possibly to V–O–Mo vibrations for polymolybdovanadate species [33,34]. For 6 wt% vanadia and higher (> 4.1 V/nm^2), bands are detected at 1000, 708, 535, 488, and 415 cm^{-1} due to crystalline V$_2$O$_5$. The fraction of V present as V$_2$O$_5$ is less than a few percent, based on the relative scattering cross sections of V$_2$O$_5$ and monovanadate and polyvanadate species [28].

The influence of precursor composition on the structure of dispersed vanadia is shown in Fig. 1b. Both spectra in Fig. 1b are for samples with vanadia loadings equivalent to one monolayer (7.5 V/nm^2) dispersed on 12Mo/Al. The principal bands seen in the sample prepared using NH$_4$VO$_3$ are those characteristic of V$_2$O$_5$ (1000, 708, 535, 488, and 413 cm^{-1}). A shoulder is also seen at 1040 cm^{-1} characteristic of monovanadate species and a band at 826 cm^{-1}, characteristic of MoO$_3$. Bands at 1016 and 775 cm^{-1}, seen in the sample prepared using vanadyl isopropoxide, are absent from the spectrum of the sample prepared using NH$_4$VO$_3$. In contrast, the sample prepared using the isopropoxide precursor shows stronger features for monovanadate (the band at 1040 cm^{-1}) and either polyvanadate or polymolybdovanadate species (the band at 775 cm^{-1}), and weaker features

shows a broad band at $\sim$ 1040 cm^{-1} characteristic of isolated monovanadate species, a broad band in the region of 700–950 cm^{-1} characteristic of polyvanadate species, and

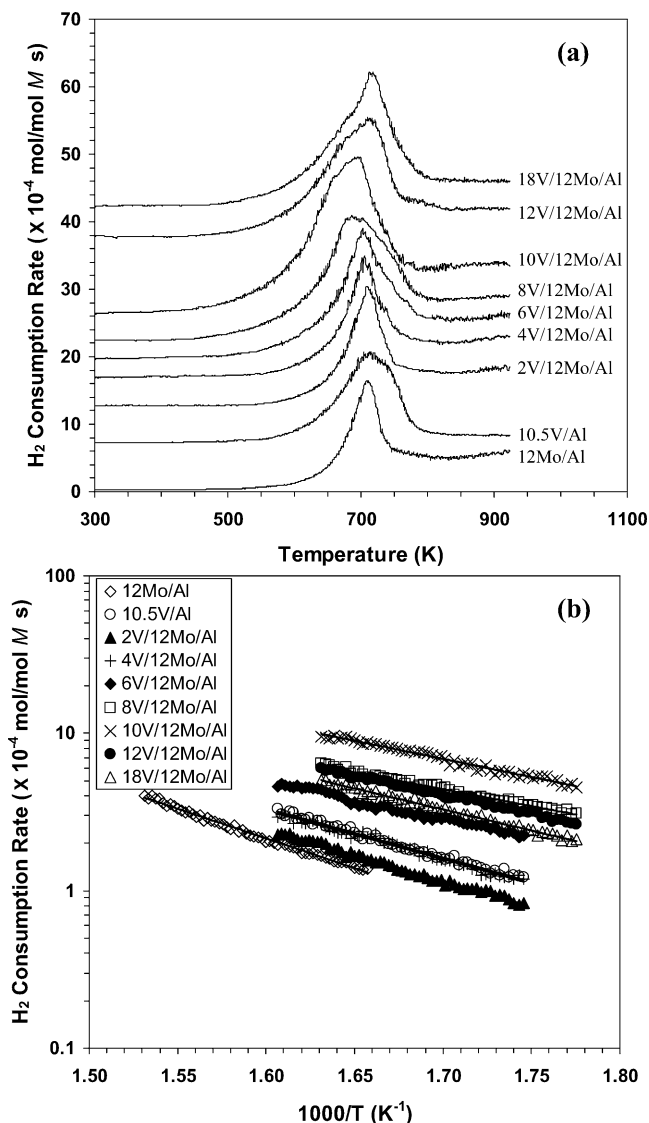Fig. 2. (a) TPR spectra of 12Mo/Al, 10.5V/Al, and xV/12Mo/Al ($x = 2$–18). (b) Arrhenius plots of the rate of H_2 consumption during TPR versus inverse temperature.

for V_2O_5. These results suggest for a given apparent surface density of vanadia, a greater fraction of the vanadia is dispersed in the form of monovanadate and polyvanadate species, and that structures involving V–O–Mo bonds may be formed when vanadyl isopropoxide is used as the vanadium precursor.

Temperature-programmed reduction (TPR) data were used in order to probe the effects of the MoO_x interlayer on vanadia reducibility and the results are shown in Fig. 2. The data for 12Mo/Al show a single reduction peak centered at about 710 K followed by a broad feature at higher temperatures. These data are similar to those previously reported [13,15]. The peak at 710 K corresponds to the reduction of Mo^{6+} to Mo^{4+}, whereas the feature at higher temperature reflects the reduction of Mo^{4+} to Mo^0 [35,36]. TPR of 10.5V/Al led to a broad asymmetric feature at about 710 K,

which has been previously attributed to the reduction of V^{5+} to V^{3+} [15]. The addition of increasing amounts of vanadia to 12Mo/Al leads to a broadening of this feature and its shape evolves to one resembling that in 10.5V/Al. Above 8 wt% (> 5.7 V/nm^2) vanadia contents, a sharp feature appears at ~ 690 K, which shifts to 720 K with increasing vanadia content. This new feature is attributed to the reduction of increasingly larger amounts of crystalline V_2O_5 [14].

The logarithm of the initial rate of H_2 reduction is plotted in Fig. 1b versus inverse temperature. For a fixed temperature, it is apparent that 12Mo/Al exhibits the lowest reduction rate and that reduction rates increase with increasing vanadia contents up to 10 wt% (7.5 V/nm^2). At higher contents, reduction rates decreased, apparently because of the lower accessibility of V atoms and the longer oxygen diffusion distances prevalent in larger three-dimensional structures. It is also evident that the rate of reduction of 10V/12Mo/Al is significantly higher than for 10.5V/Al or 12Mo/Al. These trends are qualitatively similar to those reported by Ruth et al. [37], who showed that the initial reduction temperature for bulk V_2O_5, MoO_3, and $Mo_6V_9O_{40}$ increases in the order $Mo_6V_9O_{40}$ (748 K) < V_2O_5 (773 K) < MoO_3 (848 K). Thus, it is possible that the increase in catalyst reducibility observed when VO_x is dispersed on 12Mo/Al is attributable to the formation of polymolybdovanadate species. Such an interpretation would be consistent with the assignment of the Raman band at 775 cm^{-1} to V–O–Mo vibrations (see above).

Fig. 3 shows C_3H_6 and CO_x ($CO + CO_2$) selectivities on 10.5V/Al and 10V/12Mo/Al as a function of C_3H_8 conversion at 613 and 673 K. On both catalysts, C_3H_6 selectivity decreases and CO_x selectivity increases with increasing C_3H_8 conversion over the range of C_3H_8 conversions investigated. For a given C_3H_8 conversion, 10.5V/12Mo/Al gives higher C_3H_6 selectivities than 10.5V/Al. These data show that the dispersion of vanadia on a layer of MoO_x deposited on Al_2O_3 increases the ODH selectivity of active vanadia domains. These selectivity effects are discussed later in terms of the rate constants for ODH and for primary and secondary combustion reactions.

The initial rate of propene formation (at zero propane conversion) was determined by extrapolation of propene formation rates to zero residence times [7,9–11,13,14]. Fig. 4a shows the effects of VO_x surface density on initial propene formation rates (per catalyst mass) at 613, 643, and 673 K. At each temperature, initial propene formation rates increased with increasing V surface density up to values of ~ 7–8 V/nm^2, corresponding to a theoretical polyvanadate monolayer, and then decreased at higher surface densities. Propene formation rates on 10.5V/Al are also shown in Fig. 4a. These data clearly show that propene formation rates are significantly higher when VO_x structures are deposited on a MoO_x-modified Al_2O_3 surface than when similar structures are placed on pure Al_2O_3 at apparent V surface densities corresponding to a theoretical monolayer. Areal propene formation rates (based on BET surface area) are shown in
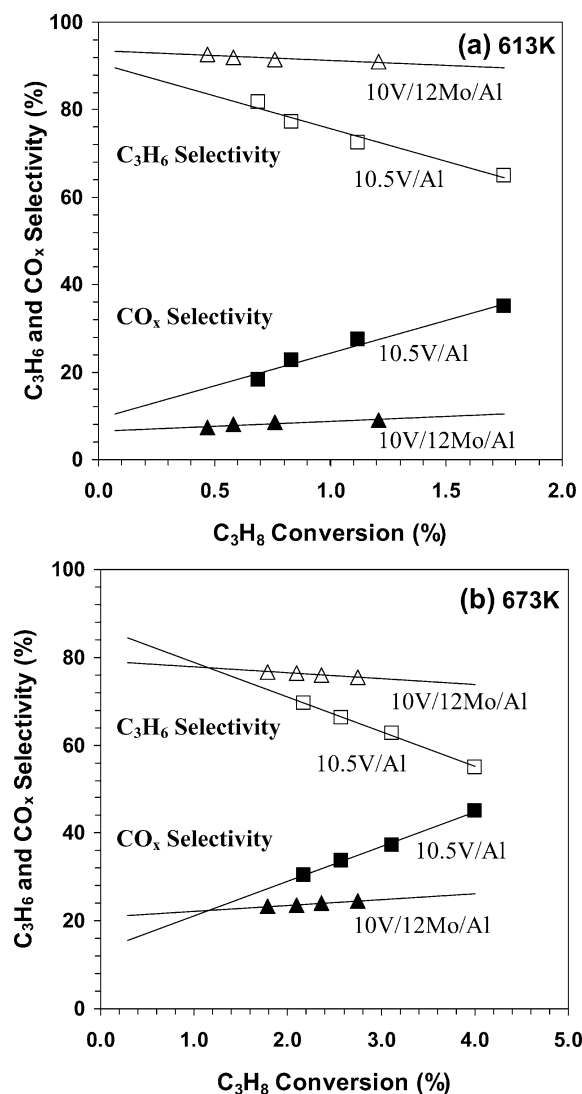
Fig. 3. Dependence of C_3H_6 and CO_x selectivities as functions of C_3H_8 conversion for (a) 613 K and (b) 673 K.
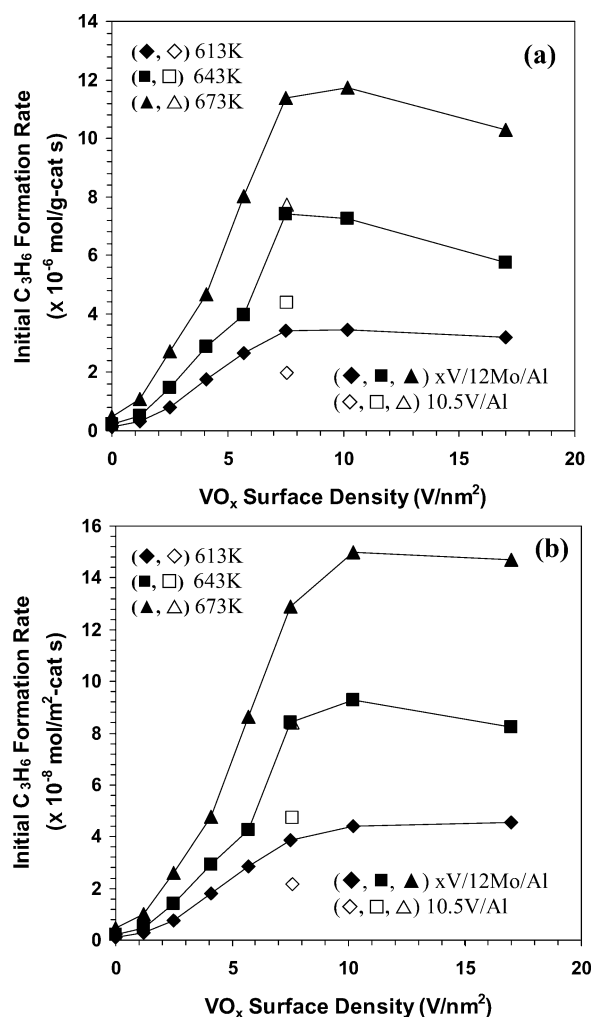

Fig. 4. Effects of VO_x surface density on the initial rates of C_3H_6 formation per gram of catalyst (a) and per unit surface area of catalyst (b).

Fig. 4b. Above 10 VO_x/nm^2, areal rates reach nearly constant values, indicating that neither the specific activity nor the amount of exposed VO_x species increased as VO_x surface densities exceed theoretical polyvanadate monolayer values.

Fig. 5a shows initial propene formation rates normalized per V atom as a function of V surface density. Since the rate of propene formation on 12Mo/Al is very small at the temperatures of the present study, no correction was made to separate the rate of propene formation on exposed MoO_x from that on VO_x. At all three temperatures, rates (per V atom) reached maximum values at surface densities of ~ 7–8 VO_x/nm^2, as also shown previously for V_2O_5/Al_2O_3 [28]. At a given V surface density, propene formation rates are 1.5–2.0 times higher when VO_x is dispersed on MoO_3/Al_2O_3 instead of on pure Al_2O_3. The trends shown for high surface densities in Fig. 5 are consistent with the expected loss of accessibility of V centers as three-

dimensional V_2O_5 structures form at apparent VO_x surface densities above 7.5 V/nm^2 (see Figs. 1 and 2).

The observed increase in specific rates with V surface density below 7.5 V/nm^2 reflects a monotonic increase in the size and reducibility of VO_x domains [15]. The UV–visible edge energy of V_2O_5/Al_2O_3 samples decreases with increasing V surface density, as a result of electron delocalization over larger VO_x domains containing V–O–V linkages. The decrease in UV–visible band-edge energy is also indicative of a greater ease of O-to-V electron transfer, a critical step in the oxidative addition of propane to vanadia structures. Since this step has been shown to be rate limiting, increasing its rate would also increase the rate of propane ODH. Fig. 1a shows a similar pattern in the change in the structure of the dispersed VO_x with increasing vanadia loading for vanadia dispersed on alumina containing a layer of molybdena as that reported for vanadia dispersed on alumina [15]. The most significant difference is the appearance of the band at 775 cm^{-1}, which grows in intensity with increasing vanadia loading. As noted earlier, the concurrent increase in the rate of H_2 reduction of vanadia deposited
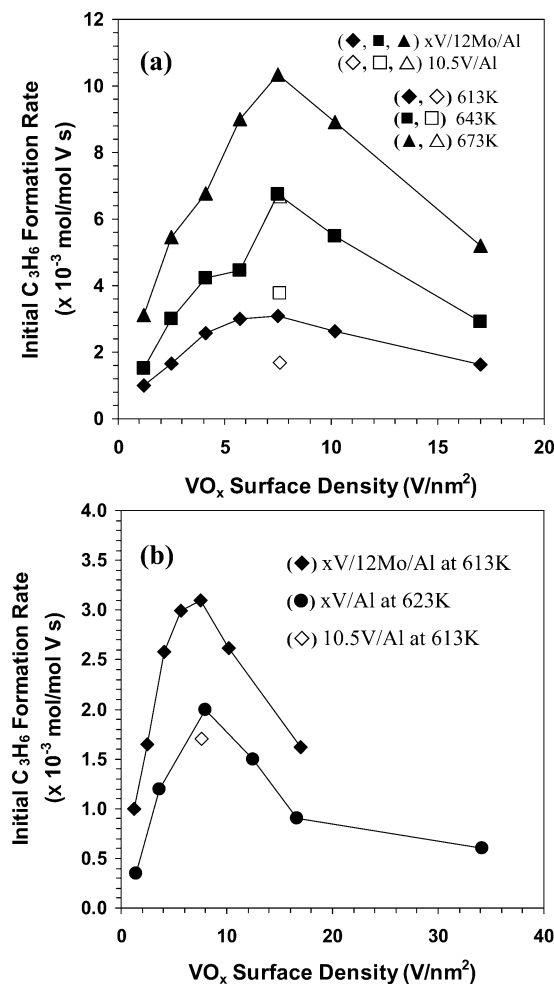
Fig. 5. (a) Effects of VO_x surface density on the rates of C_3H_6 formation per mole of V for $xV/12Mo/Al$ ($x = 2$–18) and $10.5V/Al$. (b) Comparison of the effects of VO_x surface density on the rates of C_3H_6 formation per mole of V for $xV/12Mo/Al$ ($x = 2$–18), xV/Al ($x = 2$–30), and $10.5V/Al$.

Fig. 6. Effects of VO_x surface density on the rates of H_2 consumption during TPR expressed per gram of catalyst (a) and per mole of V (b) for $xV/12Mo/Al$ ($x = 2$–18) and $10.5V/Al$.

on layers of molybdena deposited on alumina relative to that for vanadia deposited on alumina suggests that both the band at 775 cm^{-1} and the increased rate of reduction can be attributed to the formation of V–O–Mo bonds associated possibly with polymolydovanadate species. This conclusion is supported by the results presented in Fig. 6, which show that the rate of H_2 reduction (per gram or per V atom) at 613 K for $xV/M12Mo/Al$ increases with VO_x surface density up to a value of 7.5 V/nm^2 and then decreases. This pattern is similar to that seen in Figs. 4a and 5 for propene formation rates. It is also observed that at a surface density of 7.5 V/nm^2, the rate of VO_x reduction for vanadia supported on alumina is significantly lower than that for vanadia supported on alumina containing a monolayer of molybdena. This effect of the molybdena interlayer is consistent with the expected reducibility of V–O–Mo bonds compared to V–O–Al bonds.

Fig. 7a shows initial propene selectivities as a function of V surface density. At the three reaction temperatures used the initial propene selectivity is ~ 95% on the
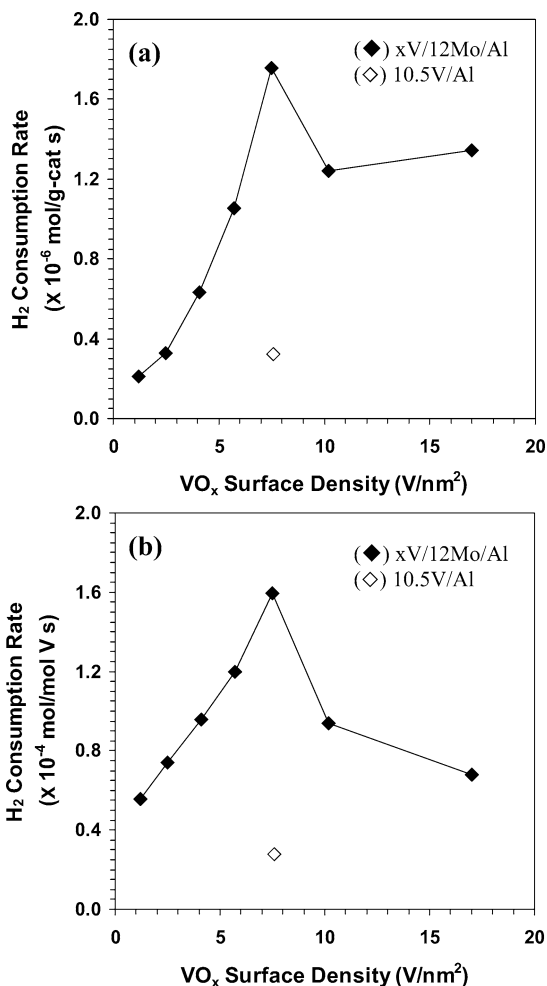
12Mo/Al material used as the support. Initial selectivities increased to 100% with the addition of small amounts of V, but then decreased monotonically for V surface densities above 2 VO_x/nm^2. At 643 and 673 K, the MoO_x interlayer did not influence initial propene selectivities, but this MoO_x interlayer, however, increased propene selectivities at 613 K. Fig. 7b demonstrates that V surface density effects are virtually identical for VO_x domains dispersed on Al_2O_3 and MoO_x/Al_2O_3 supports, but the latter give higher initial propene selectivities than Al_2O_3 supports at 613 K for all surface densities.

Previous kinetic and mechanistic studies of propane ODH on VO_x and MoO_x catalysts have shown that primary and secondary reactions can be accurately described by the scheme [1,3,4,7,9–11,13,14]:
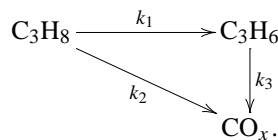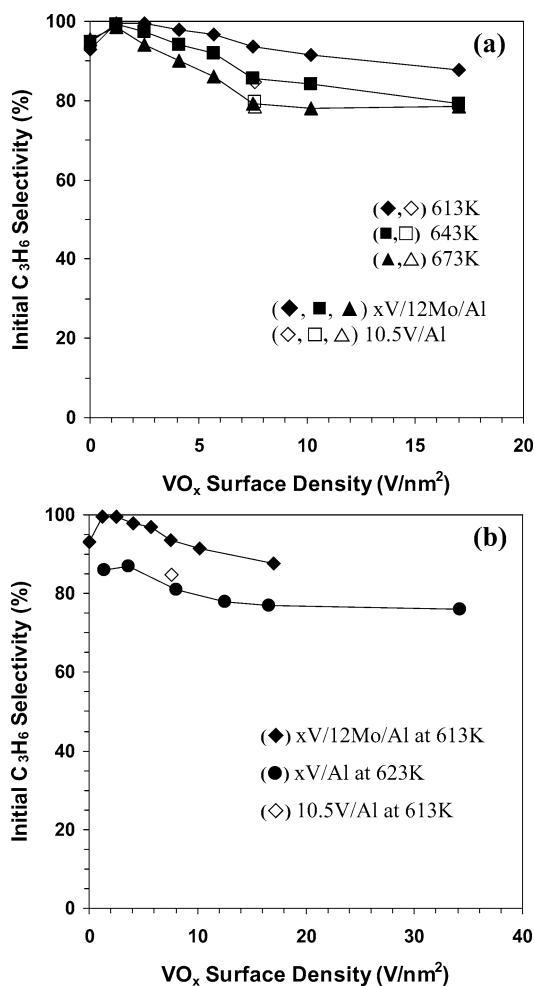
$$C_3H_8 \xrightarrow{k_1} C_3H_6 \xrightarrow{k_3} CO_x.$$
$$\underset{k_2}{\searrow} CO_x.$$

Fig. 7. (a) Effects of VO_x surface density on the initial C_3H_6 selectivities for xV/12Mo/Al ($x = 2$–18) and 10.5V/Al. (b) Comparison of the effects of VO_x surface density on the initial C_3H_6 selectivities for xV/12Mo/Al ($x = 2$–18), xV/Al ($x = 2$–30), and 10.5V/Al.

Fig. 8. (a) Effects of VO_x surface density on k_2/k_1 for xV/12Mo/Al ($x = 2$–18) and 10.5V/Al. (b) Comparison of the effects of VO_x surface density on k_2/k_1 for xV/12Mo/Al ($x = 2$–18), xV/Al ($x = 2$–30), and 10.5V/Al.

Each reaction is accurately described using pseudo-first-order dependencies on propane and propene reactants and zero order in O_2 [7,10,11]. The propane ODH rate constant (k_1) is given by the initial propene synthesis rates (extrapolated to zero residence time, τ). The direct combustion rate constant (k_2) is obtained from the C_3H_6 selectivity extrapolated to zero space time ($S^0 = k_1/(k_1 + k_2)$). Finally, propene combustion rate constants (k_3) are estimated from the measured effects of space time on propene selectivity ($S = S^0[1 - (k_3 + k_2 + k_1)C_v\tau/2]$, where C_v is the concentration of M atoms per unit reactor volume). The k_2/k_1 and k_3/k_1 ratios reflect relative rates of C_3H_8 combustion and dehydrogenation, and of C_3H_6 combustion and dehydrogenation, respectively. Small values of these ratios lead to higher propene selectivities at a given propane conversion. The k_2/k_1 ratios are typically small (0.1–0.2) [7–11,13,14] and propene selectivities and yields depend mostly on the value of k_3/k_1 ratios.

Fig. 8 shows k_2/k_1 ratios as a function of VO_x surface density. These ratios decrease with increasing VO_x surface
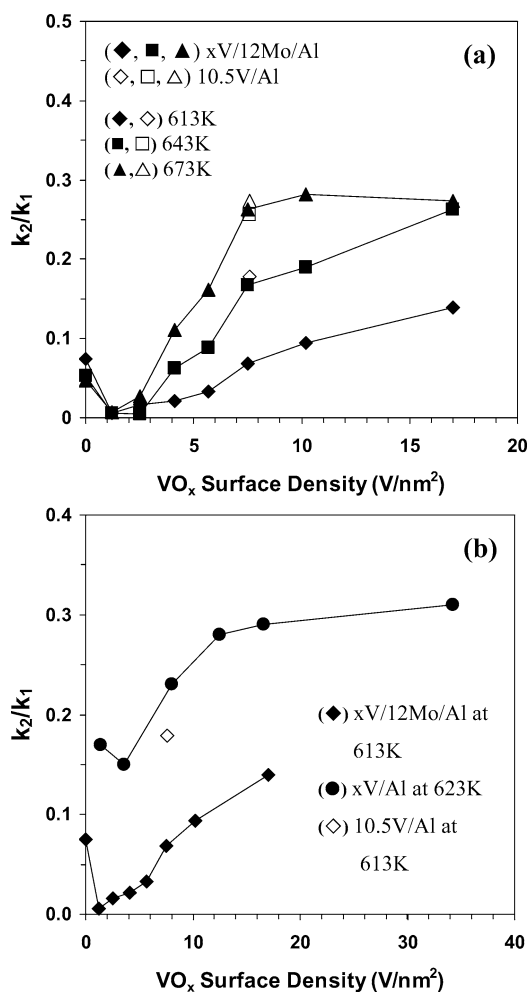
density up to ~ 2 V/nm^2 and then increase monotonically for higher surface densities. The presence of a molybdena interlayer has no effect on the value of k_2/k_1 at 673 K, but leads to a lower value of this ratio at lower temperatures (Fig. 8a). On all catalysts, k_2/k_1 ratios increased with increasing reaction temperature, indicating that the activation energy for propane combustion is higher than for ODH [14]. The k_2/k_1 ratios increased with increasing V surface density on both supports, but they were significantly lower on MoO_x/Al_2O_3 than on pure Al_2O_3 supports at all surface densities (Fig. 8b).

The influence of vanadia surface density on k_3/k_1 ratios is shown in Fig. 9a for MoO_x/Al_2O_3 supports. The k_3/k_1 ratios decrease with increasing surface density up to 7.5 VO_x/nm^2, and then increase gradually as V surface densities increases beyond this value. With increasing temperature, k_3/k_1 decreases, indicating that the activation energy for propane ODH is larger than that for propene ODH. These k_3/k_1 values are much lower for VO_x domains supported on MoO_x/Al_2O_3 than for domains supported at similar sur-
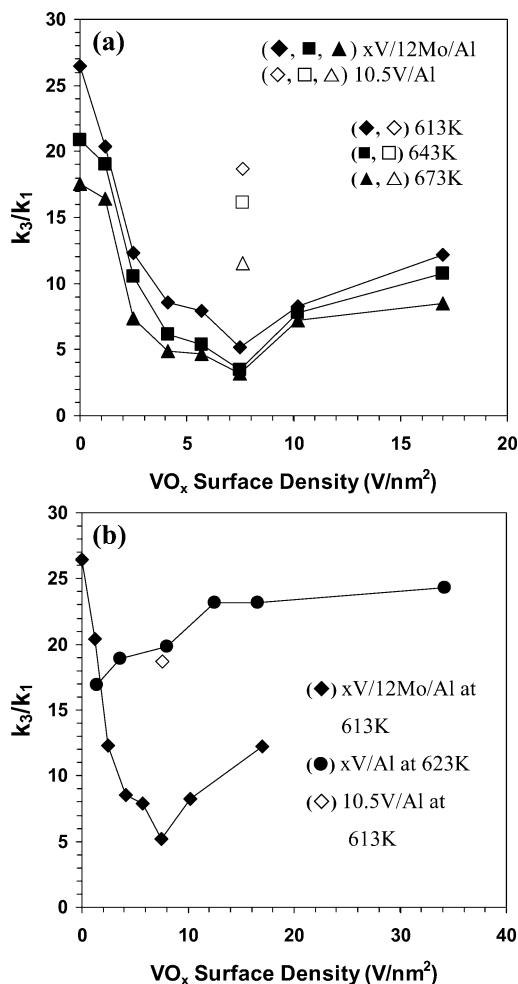
Fig. 9. (a) Effects of VO_x surface density on k_3/k_1 for xV/12Mo/Al ($x = 2$–18) and 10.5V/Al. (b) Comparison of the effects of VO_x surface density on k_3/k_1 for xV/12Mo/Al ($x = 2$–18), xV/Al ($x = 2$–30), and 10.5V/Al.

face densities on Al_2O_3 (Fig. 9b). These data indicate that the molybdenum interlayer suppresses propene combustion rates relative to propane ODH rates. The effects of vanadia surface density on k_3/k_1 ratios are shown for VO_x domains on both Al_2O_3 and MoO_x/Al_2O_3 supports in Fig. 9b. On Al_2O_3, the k_3/k_1 ratio increases monotonically with increasing vanadia surface density. The high initial value of k_3/k_1 on MoO_x/Al_2O_3 reflects a significant catalytic contribution from MoO_x domains, which show much higher k_3/k_1 ratios than VO_x domains [13,14]. As vanadia covers an increasing fraction of the exposed MoO_x surface, it reduces the contributions from the latter to combustion rates, because the specific activity of vanadia is much higher than that of molybdena [13,14]. A minimum k_3/k_1 value is achieved at a surface density of 7.5 VO_x/nm^2, which corresponds to a theoretical polyvanadate monolayer. Above a surface density of 7.5 V/nm^2, however, k_3/k_1 increases with increasing surface density as in the case of pure Al_2O_3 supports. Despite of some residual contributions from less selective MoO_x domains, VO_x domains dispersed on MoO_x/Al_2O_3 give much

lower k_3/k_1 ratios than when dispersed on Al_2O_3 at all VO_x surface densities. This appears to reflect the higher dispersion of VO_x species on MoO_x/Al_2O_3 supports than on Al_2O_3, which minimizes unselective reactions prevalent in V_2O_5 crystallites. These unselective reactions lead to the observed increase in k_3/k_1 ratios with increasing VO_x surface densities on both MoO_x/Al_2O_3 and Al_2O_3 supports. This interpretation is consistent with the observation of an increasing amount of V_2O_5 in the Raman spectra shown in Fig. 1a.

4. Conclusions

The dispersion of VO_x on alumina containing a monolayer equivalent of molybdena increases the catalyst activity (per V atom) and selectivity for propane ODH to propene. The higher activity is ascribed to the formation of V–O–Mo bonds between the dispersed vanadia and the molybdena layer. The formation of these bonds appears to be facilitated by the use of vanadyl isopropoxide as the precursor for the dispersed vanadia. Analysis of the reaction kinetics shows that the ratios of the rate coefficients for propane and propene combustion relative to propane ODH are significantly lower for vanadia supported on a monolayer of molybdena on alumina than those for vanadia supported on alumina alone. These results are unexpected and may be attributable to the presence of V–O–Mo bonds formed by reaction of the dispersed vanadia with the molybdena layer deposited on the alumina support. It is possible that these bonds are associated with the formation of polymolybdovanadate species.

References

[1] H. Kung, Adv. Catal. 40 (1994) 1.
[2] E.A. Mamedov, V. Cortes Corberan, Appl. Catal. 127 (1995) 1.
[3] S. Albonetti, F. Cavani, F. Trifiro, Catal. Rev.-Sci. Eng. 38 (1996) 413.
[4] T. Balsko, J.M. Lopez Nieto, Appl. Catal. A 157 (1997) 117.
[5] I.E. Wachs, B.M. Wechuysen, Appl. Catal. A 157 (1997) 67.
[6] L.E. Cadus, M.F. Gomez, M.C. Abello, Catal. Lett. 43 (1997) 229.
[7] A. Khodakov, J. Yang, S. Su, E. Iglesia, A.T. Bell, J. Catal. 177 (1998) 343.
[8] A. Khodakov, B. Olthof, A.T. Bell, E. Iglesia, J. Catal. 181 (1999) 205.
[9] K. Chen, S. Xie, E. Iglesia, A.T. Bell, J. Catal. 189 (2000) 421.
[10] K. Chen, A. Khodakov, J. Yang, A.T. Bell, E. Iglesia, J. Catal. 186 (1999) 325.
[11] K. Chen, E. Iglesia, A.T. Bell, J. Phys. Chem. B 105 (2001) 646.
[12] E.V. Kondratenko, M. Baerns, Appl. Catal. A 222 (2001) 133.
[13] K. Chen, S. Xie, A.T. Bell, E. Iglesia, J. Catal. 198 (2001) 232.
[14] M.D. Argyle, K. Chen, E. Iglesia, A.T. Bell, J. Catal. 208 (2002) 139.

[15] K. Chen, A.T. Bell, E. Iglesia, J. Catal. 209 (2002) 35.
[16] X. Gao, S.R. Bare, J.L.G. Fierro, I.E. Wachs, J. Phys. Chem. B 103 (1999) 618.
[17] X. Gao, J.L.G. Fierro, I.E. Wachs, Langmuir 15 (1999) 3169.
[18] X. Gao, I.E. Wachs, Top. Catal. 18 (2002) 243.
[19] W. Ueda, N.F. Chen, K. Oshihara, Chem. Commun. (1999) 517.
[20] G. Centi, Appl. Catal. A 147 (1996) 267.
[21] H. Knözinger, P. Ratnasamy, Catal. Rev.-Sci. Eng. 17 (1978) 31.
[22] Y.C. Xie, Y.Q. Tang, Adv. Catal. 37 (1990) 1.
[23] Y. Chen, L.F. Zeng, Catal. Lett. 12 (1992) 51.
[24] M.A. Vuurman, I.E. Wachs, J. Phys. Chem. 96 (1992) 5008.
[25] I.E. Wachs, Catal. Today 27 (1996) 437.
[26] B. Olthof, A. Khodakov, A.T. Bell, E. Iglesia, J. Phys. Chem. B 104 (2000) 1516.

[27] L. Abello, E. Husson, Y. Repelin, G. Luzean, Spectrochim. Acta 39A (1983) 641.
[28] S. Xie, E. Iglesia, A.T. Bell, J. Phys. Chem. B 105 (2001) 5144.
[29] S.S. Chan, I.E. Wachs, L.L. Murrell, J. Phys. Chem. 88 (1984) 5831.
[30] H. Hu, I.E. Wachs, S.R. Bare, J. Phys. Chem. 99 (1995) 10897.
[31] G. Mestl, T.K.K. Srinivasan, Catal. Rev.-Sci. Eng. 40 (1998) 451.
[32] G. Busca, G. Ricchardi, D. Siew Hew Sam, J.-C. Volta, J. Chem. Soc., Faraday Trans. 90 (1994) 1161.
[33] J.R. Regalbuto, J.W. Ha, Catal. Lett. 29 (1994) 1189.
[34] M. Cindrič, B. Kamenar, N. Strukan, Polyhedron 14 (1995) 1045.
[35] N. Strukan, M. Cindrič, B. Kamenar, Polyhedron 16 (1997) 629.
[36] P. Arnoldy, J.C.M. de Jonge, J.A. Moulijn, J. Phys. Chem. 89 (1985) 451.
[37] K. Ruth, R. Burch, R. Keiffer, J. Catal. 175 (1998) 27.